Exhibit A

REPORT DOCUMENTATION PAGE

Form Approved
OMB No. 0704-0188

1. AGENCY USE ONLY (Leave Blank)	2. REPORT DATE	3. REPORT TYPE AND DATES COVERED
	Sept. 5, 2000	Final Report

4. TITLE AND SUBTITLE
InAs/GaInSb Based Detectors Sensitive to Radiation Beyond 15um

5. FUNDING NUMBERS

6. AUTHOR(S)
Dr. Peter P. Chow

7. PERFORMING ORGANIZATION NAME(S) AND ADDRESS(ES)
SVT Associates, Inc.
7620 Executive Drive
Eden Prairie, MN 55344

8. PERFROMING ORGANIZATION REPORT NUMBER
Final

9. SPONSORING/MONITORING AGENCY NAME(S) AND ADDRESS(ES)
AFRL/MLKN
Wright Laboratory
2530 B Street
Wright-Patterson AFB, OH 45433

10. SPONSORING/MONITORING AGENCY REPORT NUMBER

11. SUPPLEMENTARY NOTES

12a. DISTRIBUTION/AVAILABILITY STATEMENT
Approved for public release; distribution unlimited

12b. DISTRIBUTION CODE

13. ABSTRACT (Maximum 200 words)

Report developed under SBIR contract for topicAF99-163. Due to the lack of availibility of suitable GaSb substrates our strategy has been to make suitable buffer layers on the semi-insulating GaAs substrates before the superlattices are grown. Although significant progress was made to produce reasonable quality (111) superlattice samples, further improvement is necessary to reach the level of the (100) superlattices. Interpretation of the measurement result is thus in part affected by the relatively high level of defects in these samples, and decisive comparison can not yet be made between the two crystalline orientations. Nonetheless a systematic study has been carried out which resulted in producing bandedge transmission as long as 15 um. Many samples exhibiting 8-12 um have been demonstrated. We are hopeful with improving growth techniques the theoretical prediction for these (111) superlattices may be realized.

14. SUBJECT TERMS	15. NUMBER OF PAGES
Superlattice, VLWIR, bandedge, (111)	25
	16. PRICE CODE

17. SECURITY CLASSIFICATION OF REPORT	18. SECURITY CLASSIFICATION OF THIS PAGE	19. SECURITY CLASSIFICATION OF ABSTRACT	20. LIMITATION OF ABSTRACT
Unclassified	Unclassified	Unclassified	Unlimited

InAs/GaInSb Based Detectors Sensitive to Radiation Beyond 15 um

Contract # F33615-99-C-5419

Dr. David Tomich
Technical Monitor

Final Report

Submitted to:

AFRL/MLPO Bldg. 651
3005 P Street, Ste 6
Wright-Patterson AFB, OH 45433-7707

PI: Peter P. Chow

SVT Associates, 7620 Executive Drive, Eden Prairie, MN 55344

Phase I **Contract # F33615-99-C-5419**

Title **InAs/GaInSb Based Detectors Sensitive to Radiation Beyond 15 um**

1.0 Introduction

The objective of this Phase I project is to develop very long wavelength infrared (VLWIR) detector by fabricating InAs/GaInSb strained-layer superlattices on the (111) oriented substrates. This class of superlattice has been proposed to have the potential to exceed the performance of HgCdTe, the current inrared detector of choice, due to larger electron effective mass and much longer Auger lifetime. These advantages become more significant at longer wavelengths.

These materials normally align in a type-II band configuration, with electrons localized in the InAs layers and holes in the $In_xGa_{1-x}Sb$ layers. In a strained layer superlattice structure, an engineered band is created which provides good absorption coefficients for long-wavelength IR light. The lattice constants for InAs and $In_xGa_{1-x}Sb$ layers are smaller and larger, respectively, than that of GaSb substrate. Thus, the alternating thin layers of this superlattice can be applied such that the overall lattice mismatch is compensated. This in turn can result in thick layers of the superlattice which are defect- and dislocation- free.

Much of the previous exploration into this topic has been performed using (100)-oriented substrates. Like all zincblende structures of the III-V semiconductors these superlattices are piezoelectric with the largest effect along the (111) orientation. The fields cause a tilting of the energy bands, so the heavy hole mass along the [111] direction is larger than in the [100]. The quantum confinement energy for the holes is lowered and it can result

in a higher absorption coefficient. Furthermore, the piezoelectric fields in the [111] direction are thought to red-shift the superlattice band gap, extending the operating regime further out into the IR. Therefore, growth of the $In_xGa_{1-x}Sb/InAs$ superlattice on (111)-oriented substrates is of great interest. Despite these potential advantages little has been reported in their experimental properties due to difficulties in growing the materials along this crystalline orientation. It is the goal of this project to establish good growth methods for such superlattices so that their intrinsic performance advantages may be realized.

We have carried out nearly a hundred growth runs for this project. About 30-40 of these runs are for calibration and buffer layer growth. About 60 superlattice runs have been grown and the samples were characterized for the right combination of structural parameters to produce high quality materials. The variables are buffer layer type, In composition and thickness ratio of the constituent layers. Appropriate buffers were incorporated under the superlattice structures to balance the overall strain in the structure. In- content as high as 70% of the alloy layer can be fabricated, although the quality degraded gradually as the In percentage exceeded 50%. Many of them displayed bandedge transimission around 10 μm, and sample displaying 15 μm cutoff wavelength has been demonstrated. A partial list of the superlattice samples is presented in Table 1. We are hopeful with improving growth techniques the theoretical prediction for these (111) superlattices may be realized.

2.0 Project Summary

We have performed a thorough investigation of the growth process of (111) InAs/GaInSb superlattices. Due to lack of semi-insulating and transparent GaSb substrates we have used GaAs wafer as the substrates for growth. Several series of the InAs/GaInSb superlattices have been characterized for their crystalline, electrical and optical properties. Superlattices showing transmission edge to nearly 15 μm have been demonstrated.

Significant accomplishments achieved during this Phase I project are summarized below:

- High quality buffer layer has been grown on GaAs (111) substrates
- The growth process of (111) InAs/GaInSb superlattices have been investigated
- Bandedge as long as 15 μm has been shown by FTIR transmission measurement
- P-i-n diodes along (111) orientation have been shown to show similar doping behavior as those along the (100)

3.0 Growth Process

(111)-oriented GaSb substrates are extraordinarily expensive, and are not yet available in semi-insulating form which is necessary to reduce free carrier absorption. We therefore chose to pursue this superlattice growth on (111)-oriented GaAs wafers. These substrates are commercially available in both doped and semi-insulating forms at a reasonable cost. An added benefit of using GaAs wafers is their compatibility with mature GaAs processing technology. It may be possible to combine GaAs-based electronics with the superlattice detector monolithically on the same wafer. Of course the lattice mismatched hetero-epitaxy adds to the complexity of the structure, so we undertook an investigation of individual layer growth before attempting the superlattices.

3.1 Buffer GaSb, and InAs and GaInSb layer growth

GaSb buffer layers have been grown on the GaAs substrates in both the (100) and (111) orientations. For the initial phase of this study, we also examined the growth of the individual constituents of the superlattice, GaInSb and InAs.

The MBE system is equipped with both As- and Sb-valved crackers. For mixed group-V superlattices and compounds, the flux control of the V-elements and the growth temperature are critical elements in the growth process. We characterized the flux versus valve position for both the As (Fig. 1) and Sb (Fig. 2) crackers. Such data can be applied to a computer automation of the group-V fluxes to improve the critical interfaces of the GaInSb/InAs superlattice. The linearity of the flux in this regime will aid in real-time adjustment during growth.

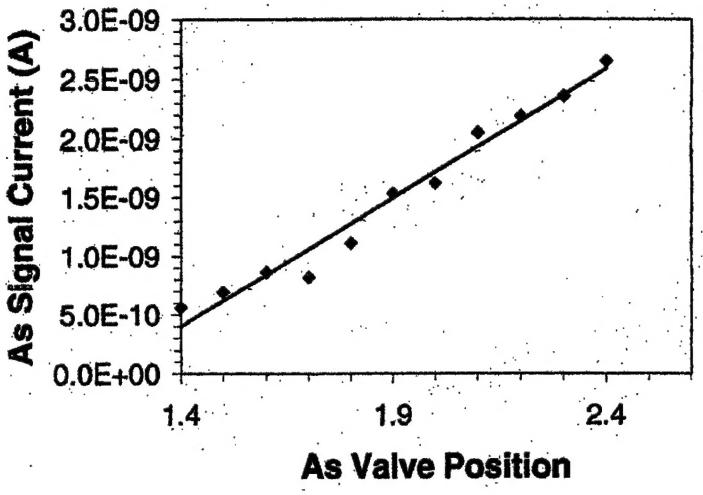

Fig. 1. As valved cracker signal versus valve position.

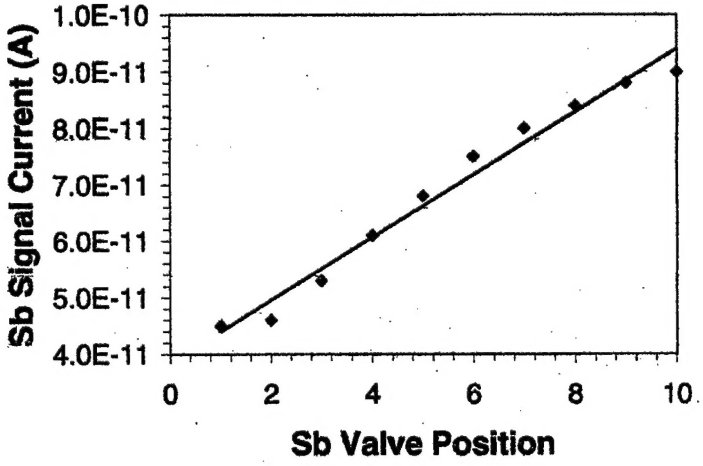

Fig. 2. Sb valved cracker signal versus valve position.

A pyrometer/reflectometer apparatus for monitoring of substrate temperature and layer thickness. In growths of test layers, we have found an improved run-to-run consistency through the temperature feedback provided by this instrument. The lower temperature limit of this pyrometer is ~ 380 °C, which is in the range of our expected growth temperature for the superlattice. This pyrometric data are used in conjunction with the RHEED observations, where the RHEED pattern for GaSb undergoes a phase change at a known and precise temperature.

The instrument, manufactured by our company as a product with the model number In-Situ 4000 (IS4K), utilizes active LED light to measure the reflectivity in real time which is then used to adjust the value of the changing emissivity of the growing layer. Such active pyrometry thus can provide much more accurate temperature readings of the substrate. The optical interference of the reflectivity measurement can be used for thickness calculations. By using two LED's of different wavelengths we can compute the refractive index of the growing layer as well. It is well known that there is significant temperature rise when small bandgap material is grown on the substrate. For InAs or GaSb on substrate the temperature rise could be as many as 60-100 degrees. The IS4K active pyrometer instrument is therefore very useful in determining the real substrate temperature.

The wafer was prepared prior to growth using a hydrochloric acid etch and deionized water rinse. The oxide on the surface was thermally desorbed at ~560 °C under an arsenic overpressure, after which the substrate temperature was lowered to ~ 500 °C for GaSb growth. No GaAs buffer layer was used. Growth conditions for the GaSb layers on (111)-A and -B were found to be about the same. Figure 1 shows the RHEED pattern during the growth of 0.74 μm of GaSb directly on (111B) GaAs substrate. X-ray rocking curves (Fig. 2) showed good quality GaSb epilayers with full-widths at half maximum (FWHM) values of ~0.14°, comparable to the GaAs substrate FWHM of ~0.13°.

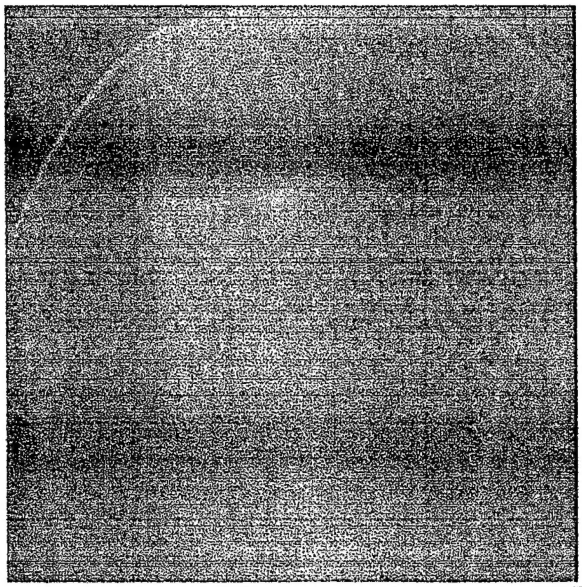

Figure 1. RHEED pattern of GaSb on <111>-A GaAs substrate

a)

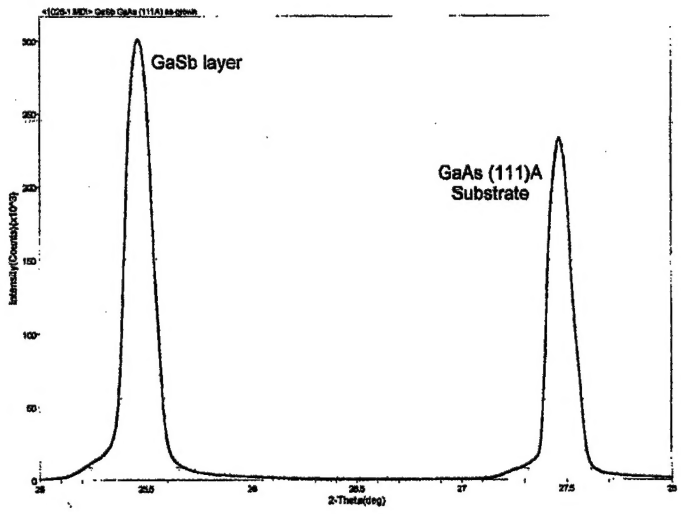

b)

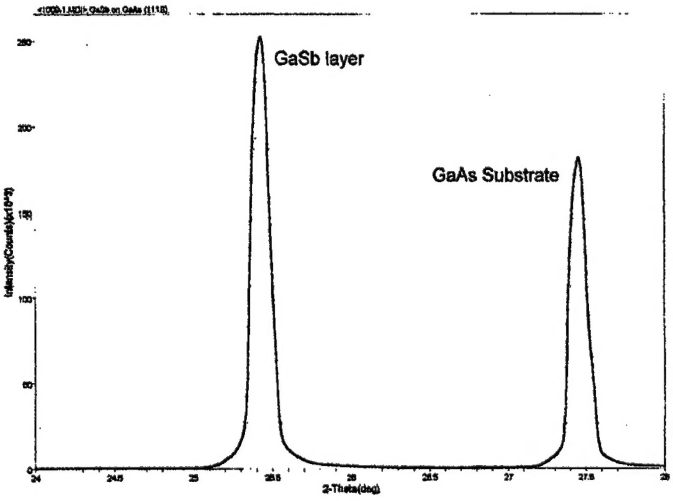

Figure 2. X-ray diffraction curves for GaSb growth on a) (111A) and b) (111B) GaAs substrates.

Atomic force microscopy was used to further investigate these GaSb on (111) GaAs layers. Figure 3 shows the AFM image of the bare (111A) GaAs wafer prior to growth. The average surface roughness is measured to be 1.8 nm. Figure 4 shows the GaSb on (111B) surface with an average roughness of 0.97 nm. Some areas are marked by aligned, parallel ridges, evidence of direction dependent preferential growth rates. A thicker GaSb buffer and refinement of the growth conditions should result in an even smoother surface for the superlattice to be deposited on.

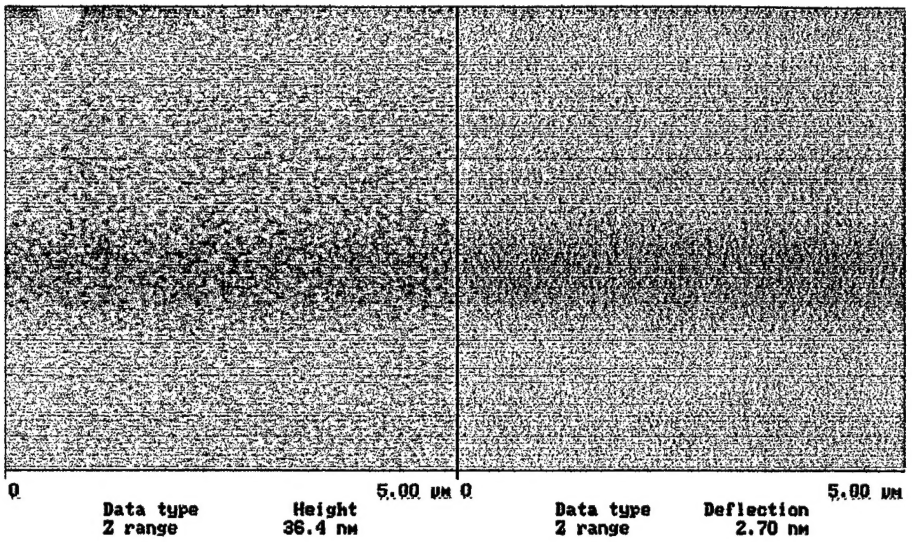

Figure 3. Atomic force microscopy (AFM) image of bare (111A) GaAs substrate prior to growth.

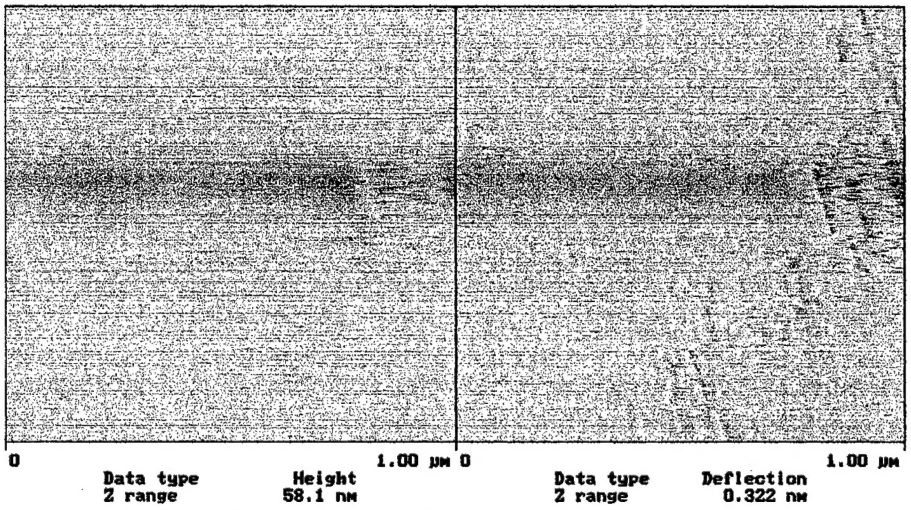

Figure 4. AFM image of 0.74 µm GaSb layer grown on (111B) GaAs substrate.

As part of the development for the superlattice, we investigated the growth of its constituent layers, InAs and $In_xGa_{1-x}Sb$, on (111) substrates. InAs growth on both A and B orientations was achieved (Figs. 5 & 6), with a FWHM value as low as 0.109° for InAs on GaAs (111A). In these cases again no buffer layer was used between the substrate and the InAs epilayers. Figure 7 displays the AFM image of the InAs on (111B), with an average roughness of 1.4 nm.

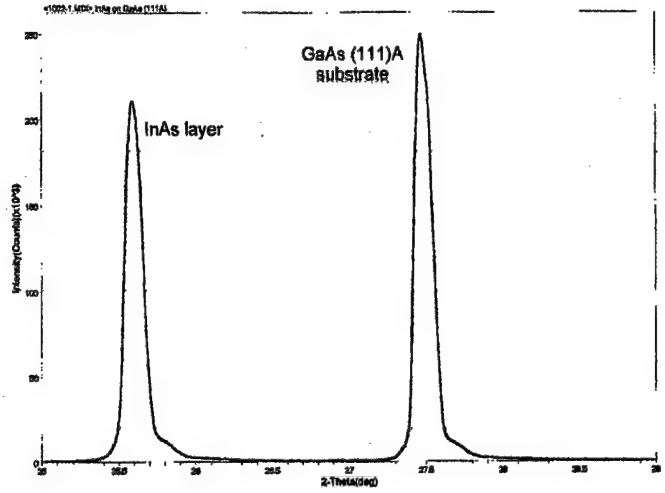

Figure 5. X-ray diffraction curve for InAs growth on (111A) GaAs.

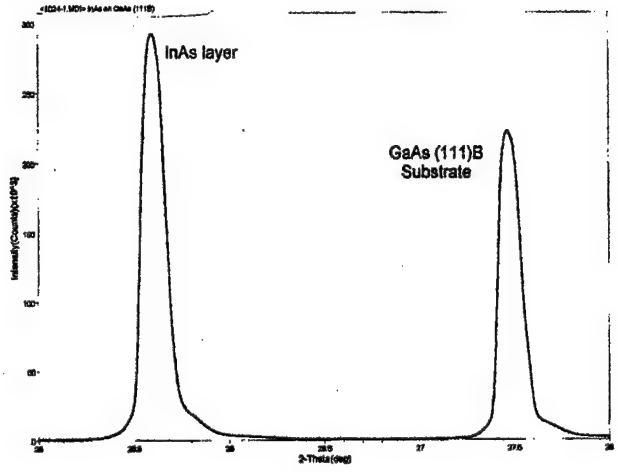

Figure 6. X-ray diffraction curve for InAs growth on (111B) GaAs.

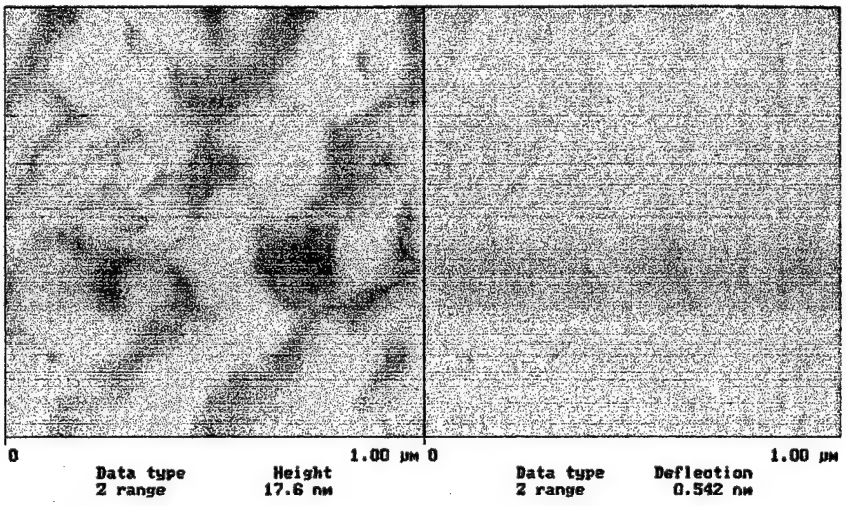

Figure 7. AFM image for InAs growth on (111B) GaAs substrate.

The next step was to combine InAs and GaSb layers on top of (111) GaAs. Here, the GaSb would act as a buffer layer between the GaAs substrate and the InAs epilayer. Figure 8 shows the X-ray diffraction of one of these samples, consisting of (111A) GaAs substrate, a 1.4 µm GaSb buffer, and a 0.8 µm InAs layer. The peaks of InAs and GaSb are shown to be clearly resolved. These experiments established the use of GaSb as a buffer upon which additional epilayers could be grown on these (111) substrates.

Because of its ternary nature, the $In_xGa_{1-x}Sb$ growth is more involved than the binary InAs layers. The In and Ga fluxes were calibrated by measuring the RHEED intensity oscillations of GaAs and InAs growth on (100) GaAs substrate, at temperatures of 580 and 470 °C, respectively. The lower growth temperature of the $In_xGa_{1-x}Sb$ alloy (from 350 to 450 °C) and the use of thermally cracked Sb species may affect our composition calibration. Our target material was $In_{0.25}Ga_{0.75}Sb$, and we found that the In/Ga ratio of our initial growths was ~5-7% higher than expected. That is, the ternary layers contained slightly more In and/or slightly less Ga than designed. Factoring this data into our calibration procedure, we can now reproducibly create our target alloy composition (Fig. 9).

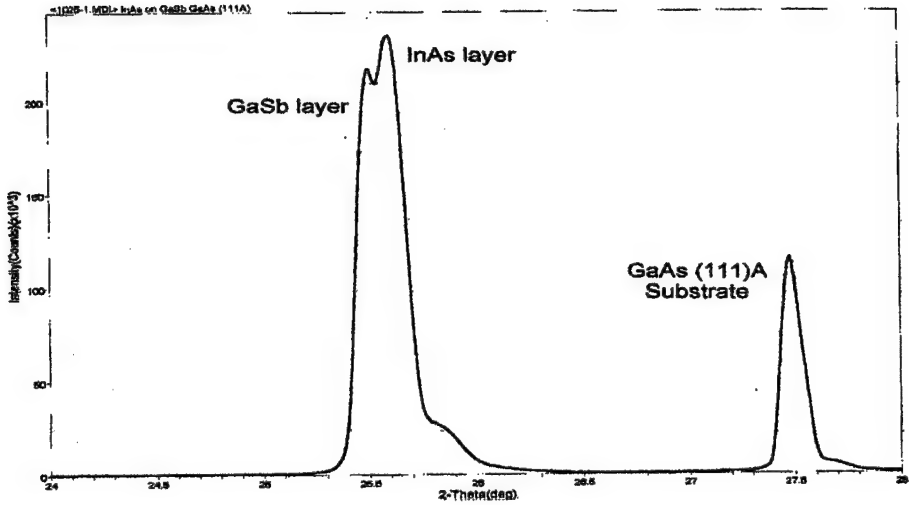

Figure 8. X-ray diffraction curve for InAs growth on (111A) GaAs substrate using a GaSb buffer layer.

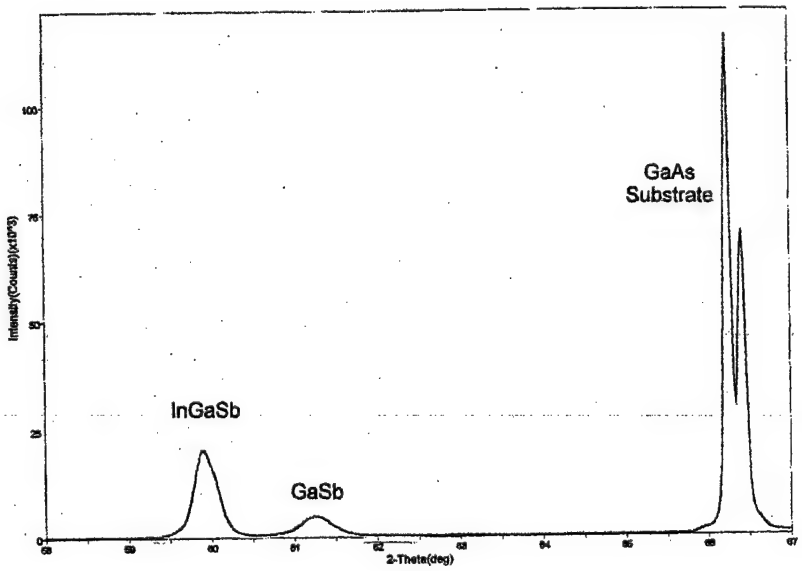

Fig. 9. X-ray diffraction curve of the InGaSb alloy grown on (100)-oriented GaAs substrate using a GaSb buffer layer

Experiments were carried out to investigate the various growth parameters for this layer using the GaSb buffer and (111) GaAs substrates. Figure 10 displays the x-ray curve for 0.7 μm $In_{0.13}Ga_{0.87}Sb$ with a 0.7 μm GaSb buffer layer on (111B) GaAs. The FHWM of the peaks were 0.13, 0.131, and 0.11° for the $In_{0.13}Ga_{0.87}Sb$, GaSb, and GaAs layers,

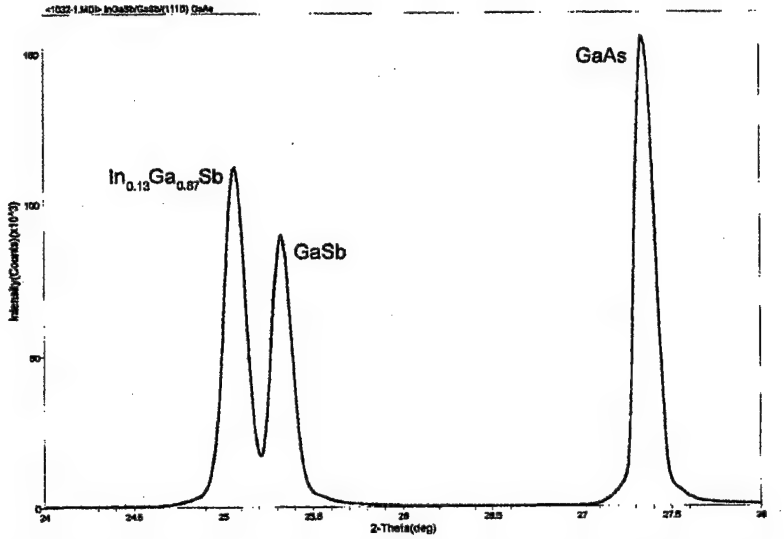

Figure 10. X-ray curve for $In_{0.13}Ga_{0.87}Sb$ on (111A) GaAs with a GaSb buffer.

respectively. Additional samples were grown with a higher In content. Figures 11 shows the $In_{0.17}Ga_{0.83}Sb$ ternary on top of 0.52 μm GaSb buffer on (111B) GaAs. The scans in Figures 10 and 11 appear almost identical and both show sharp alloy peak

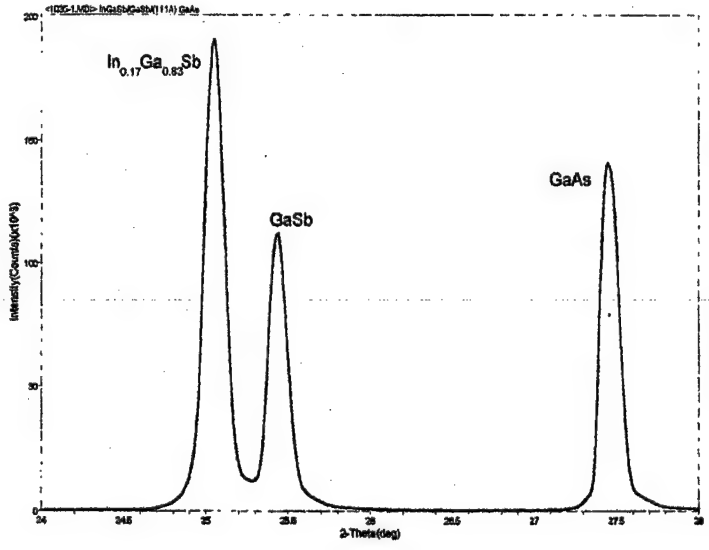

Figure 11. X-ray curve for $In_{0.17}Ga_{0.83}Sb$ on (111B) GaAs with a GaSb buffer.

We have thus established that we can grow good quality GaSb buffer layers on top of both (111A) and (111B) GaAs substrates. This process can serve as a substitute for (111)-oriented GaSb substrates which are prohibitively expensive and not readily available. We have also achieved growth of the constituent layers that comprise the superlattice, InAs and $In_xGa_{1-x}Sb$.

3.2 Superlattice Growth and Characterization

A total of about 60 superlattice runs have been grown and characterized in seeking the right combination of structural parameters to produce high quality materials that show potential of VLWIR applications. The variables are buffer layer, In composition in the alloy layer of the superlattice, and the thickness ratio of InAs and GaInSb alloy. In particular the In composition has been varied from 15% to as much as 70%. Appropriate buffer layers were incorporated under the superlattice layers to adjust the overall strain in the structure. It has been shown that even with very high In content superlattice structures can still be fabricated, albeit the quality degrades gradually as the In percentage exceeds 50%. For each In composition various thickness ratio was attempted to investigate the changes in bandgap which was determined from FTIR transmission measurement at ambient and LN2 temperatures. Many of them displayed bandedge transimission around 10 μm, although there is indication that in some cases the high defect level in these (111) structures play significant role. A partial list of these superlattice samples are summarized in Table 1.

Table 1. Summary of Superlattice Sample Growth

ID	Substrate	Composition	Pairs	FTIR	Comments
1043	111A GaAs	In.25Ga.75Sb/InAs	20/8 x 80		superlattice, abrupt shuttering
1044	111A GaAs	In.25Ga.75Sb/InAs	20/8 x 80		
1045	111A GaAs	In.25Ga.75Sb/InAs	1.5/5 x 80		
1046	111B GaAs	In.25Ga.75Sb/InAs	1.5/5 x 80		
1052	111A GaAs	In.25Ga.75Sb/InAs	1.5/3.7 x 100		
1053	111B GaAs	In.25Ga.75Sb/InAs	1.5/3.7 x 100		
1054	100 GaAs	In.25Ga.75Sb/InAs	8/20 x 60		5 sec Sb flux before each layer,
1055	111A GaAs	In.25Ga.75Sb/InAs	8/20 x 60		
1056	100 GaAs	In.37Ga.63Sb/InAs	5/12 x 80		
1057	111A GaAs	In.37Ga.63Sb/InAs	4/10 x 80		
1061	100 GaAs	In.25Ga.75Sb/InAs	8/20 x 60		
1062	111A GaAs	In.25Ga.75Sb/InAs	8/20 x 60		
1063	100 GaAs	In.25Ga.75Sb/InAs	8/15 x 60		
1064	111A GaAs	In.25Ga.75Sb/InAs	8/15 x 60		
1065	100 GaAs	In.35Ga.65Sb/InAs	6/12 x 100		
1066	111A GaAs	In.35Ga.65Sb/InAs	6/12 x 100		
1071	100 GaAs	In.3Ga.7Sb/InAs	12/12		p-i-n doped superlattice
1075	100 GaAs	In.19Ga.81Sb/InAs	8/8 x 80		
1076	100 GaAs	In.19Ga.81Sb/InAs	8/8 x 80		
1077	100 SI GaAs	In.24Ga.76Sb/InAs	8/8	8.5 um	
1078	111A SI GaAs	In.24Ga.76Sb/InAs	8/8	5.5 um	
1079	100 SI GaAs	In.24Ga.76Sb/InAs	10/10	8.5 um	
1080	111A SI GaAs	In.24Ga.76Sb/InAs	10/10	8.5 um	
1086	111A n-GaSb	In.24Ga.76Sb/InAs	10/10		
1087	111A n-GaSb	In.24Ga.76Sb/InAs	10/10		
1089	111A n-GaSb	In.34Ga.66Sb/InAs	10/10		
1090	100 SI GaAs	In.4Ga.6Sb/InAs	12/12	not sure	
1091	111A SI GaAs	In.4Ga.6Sb/InAs	12/12	9.6 um	
1092	100 SI GaAs	In.38Ga.72Sb/InAs	10/10	not sure	
1093	111A SI GaAs	In.36Ga.64Sb/InAs	10/10	~ 10 um	
1094	111A SI GaAs	In.4Ga.6Sb/InAs	10/10	~ 10 um	
1095	111A SI GaAs	In.4Ga.6Sb/InAs	6/6	~ 10 um	
1096	111A SI GaAs	In.35/Ga.65Sb/InAs	10/10	~ 10.5 um	5 s As after InAs layer, 5 sec Sb after GaIN layer
1097	111A SI GaAs	In.35/Ga.65Sb/InAs	10/10	~ 10.5 um	5 s As before InAs layer, 5 s Sb before GaI layer
1103	111A SI GaAs	In.47Ga.53Sb/InAs	8.8	~ 10 um	had 4/4 buffer superlattice
1104	111A SI GaAs	In.48Ga.52Sb/InAs	8/8	~ 11 um	In.15Ga.85Sb buffer
1105	111A SI GaAs	In.48Ga.52Sb/InAs	4/4	~ 10 um	In.15Ga.85Sb buffer
1106	111A SI GaAs	In.47Ga.53Sb/InAs	6/8	~11 um	In.15Ga.85Sb buffer
1107	111A SI GaAs	In.47Ga.53Sb/InAs	6/8	~ 11 um	As 2 sec -> InAs -> pause 2 sec -> Sb 2 sec >InGaSb -> pause 2 sec
					In.36Ga.64Sb buffer
1109	111A SI GaAs	In.7Ga.3Sb/InAs	5/7	11 um?	As 2 sec -> InAs -> pause 2 sec -> Sb 2 sec >InGaSb -> pause 2 sec

					In.36Ga.64Sb buffer
1110	111A SI GaAs	In.7Ga.3Sb/InAs	5/5	11 um?	As 2 sec -> InAs -> pause 2 sec -> Sb 2 sec >InGaSb -> pause 2 sec
					In.36Ga.64Sb buffer
1111	111A SI GaAs	In.7Ga.3Sb/InAs	8/8	11 um?	In.36Ga.64Sb buffer, 5 sec Sb soak
1112	111A SI GaAs	In.7Ga.3Sb/InAs	7/5	9.5 um	In.36Ga.64Sb buffer
1113	111A SI GaAs	In.7Ga.3Sb/InAs	7/5	8 um	In.36Ga.64Sb buffer, cooler temp than 1112
1124	111A SI GaAs	In.4Ga.6Sb/InAs	9/9 x90		
1125	111A n-GaSb	In.39Ga.61Sb/InAs	8/8 x120		p-i-n superlattice
1126	111A n-GaSb	In.39Ga.61Sb/InAs	8/8 x120		p-i-n superlattice
1173	111A SI GaAs	In.4Ga.6Sb/InAs	8/8 x 80		
1174	111A SI GaAs	In.4Ga.6Sb/InAs	8/8 x 80		
1204	111A SI GaAs	In.25Ga.75Sb/InAs	8/20 x 50	15 um?	
1205	111 1deg off-axis GaAs	In.25Ga.75Sb/InAs	8/20 x 50		
1209	111B SI GaAs	In.45Ga.55Sb/InAs	10/10 x 70		

The superlattice samples involved depositing GaSb or InGaSb buffer layers on (111)-oriented semi-insulating GaAs substrate whose semi-insulating nature facilitates optical and electrical measurement. Figure 12 displays the x-ray rocking curve of the 60 pair InAs/$Ga_{0.75}In_{0.25}Sb$ superlattice grown on (111) GaAs, where the constituent layer thicknesses were 20 and 8 monolayers, respectively. Fifth order satellite peaks can clearly be seen as well as the GaSb buffer layer peak. For this sample, a 5 second flux of Sb was applied at each interface to promote smoothness and GaSb-like interfacial ordering. Such X-ray diffraction results are comparable to the best reported in the literature, but they are still substantially inferior to those grown on the (100) substrates.

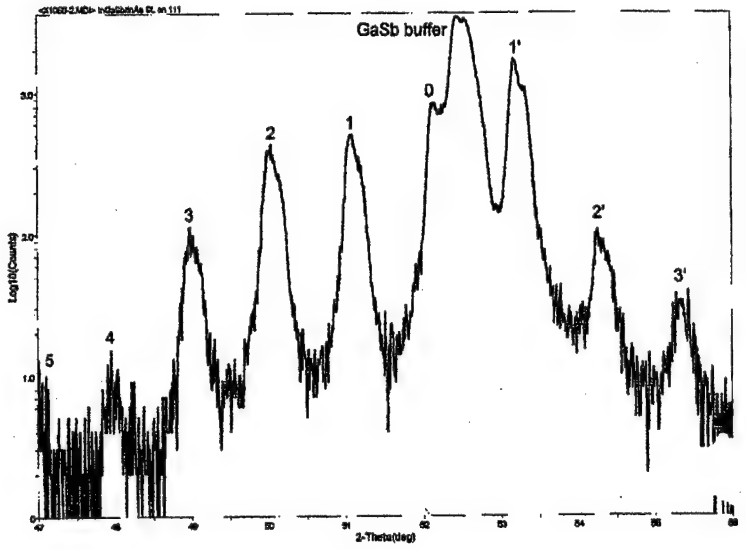

Figure 12. X-ray rocking curve for the 60 pair InAs/$Ga_{0.75}In_{0.25}Sb$ superlattice grown on (111) GaAs.

A typical optical measurement is shown in Figure 13 which displays the 300 K FTIR profile of an InAs/$Ga_{0.76}In_{0.24}Sb$ superlattice on (111) GaAs using 10 monolayer / 10 monolayer pairings for a total of 60 periods. The In composition and layer thicknesses were conservative with respect to inducing strain. Some optical interference effects are observed in the transmission spectra, but the cutoff wavelength can be estimated to be at approximately 10 μm. Theoretical modeling of this composition and thickness superlattice on (100) substrate predict a cutoff wavelength of ~ 7 μm.

Electrical measurement has been performed on some samples. Two nominally identical, unintentional doped superlattice samples, one on (100) and one (111) orientation, were sent to Wright Laboratory for electrical measurement. Figure 14 showed the temperature dependent mobility results of the samples. Qualitatively the (100) samples exhibited more temperature dependence than the (111) sample, possibly due to the fact in the latter the electrical characteristics was influenced by the high active defect level in the layer.

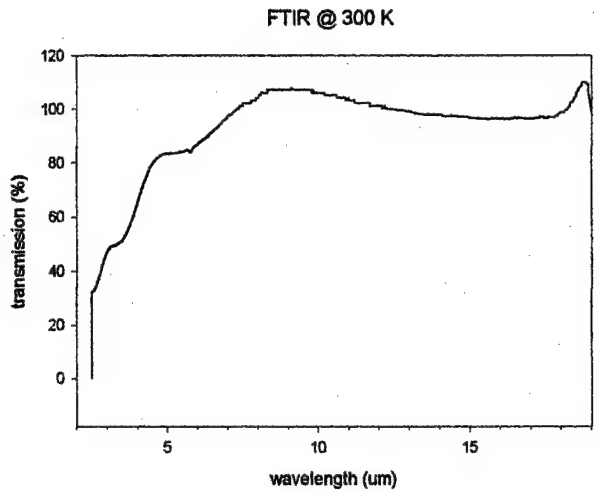

Figure 13. 300 K FTIR spectra of an InAs/$Ga_{0.76}In_{0.24}Sb$ superlattice on (111) GaAs.

The mobility of the (100) samples appeared quite good and certainly could be improved if grown on GaSb substrate. Samples with this mobility would be adequate for infrared detector operation. This verifies that our growth procedure is capable of producing good quality materials.

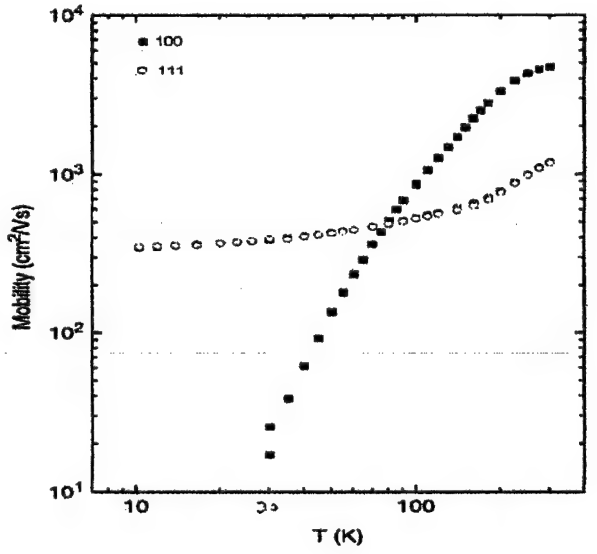

Figure 14. Temperature dependent mobility measurement of two superlattice samples of the structure 10/10 $In_{0.24}Ga_{0.76}Sb$/InAs grown on (100) and (111) GaAs respectively. Measurement courtesy of Dr. Gail Brown and Dr. Adam Saxler, Wright Laboratory.

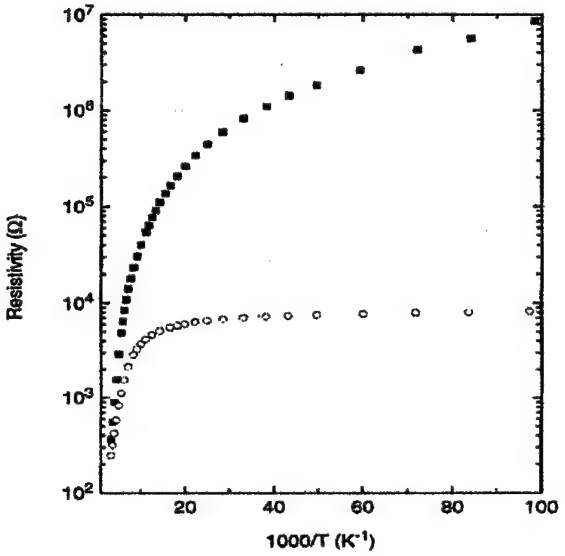

Figure 15 . Resistivity of the two samples, measurement courtesy of Dr. Gail Brown and Dr. Adam Saxler, Wright Laboratory.

Figure 15 displays the resistivity of the samples. The (111) samples showed much lower value, again possibly due to the leakage through the defects in the sample. Overall we believe the GaAs substrates can provide reasonable quality superlattice samples for investigation, but more work is needed to improve the (111) quality.

Superlattice photodiodes have been fabricated for the first time, after separate doping experiments were performed. N-type doped GaSb (111) substrates were used to study the I-V characteristics of a p-i-n doped superlattice. InAs/$Ga_{0.74}In_{0.26}Sb$ superlattice (with 10 monolayers thickness for each constituent layer) was grown on this substrate. Te and Be were used for n- and p-type doping, respectively. The thickness of the p-i-n regions is 2000/2000/3000 Å, respectively. Current-voltage (I-V) tests were conducted utilizing front side InZn dots and backside In contacts on small, cleaved portions of the sample. This p-i-n doped (111) superlattice exhibited diodic characteristics (Fig. 16). The diode exhibited softer reverse breakdown and higher forward cut-on voltage at low temperature. As far as we know this is the first time superlattice diode structures have been fabricated in the (111) orientation.

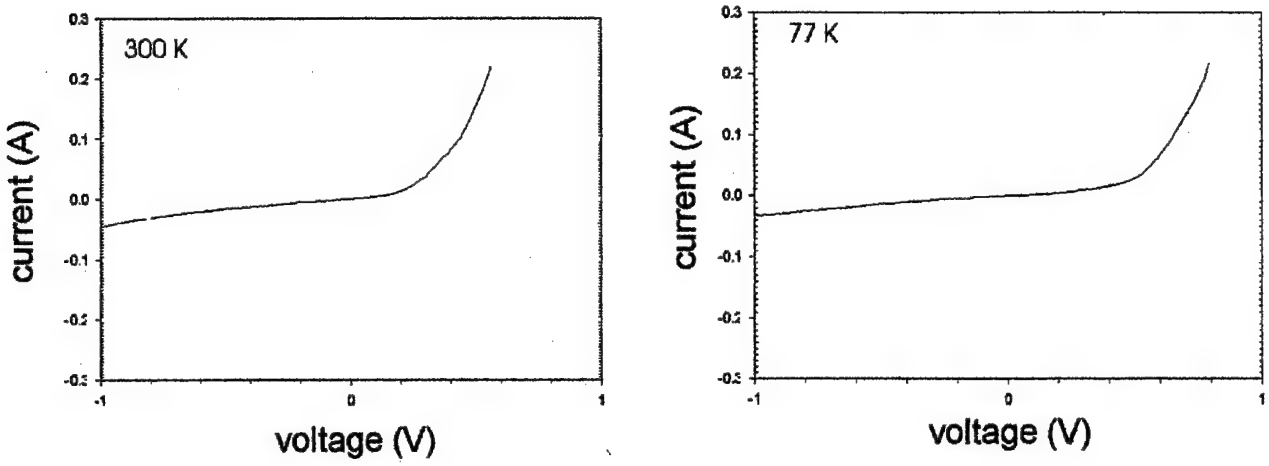

a) b)

Figure 16. I-V characteristic for InAs/$Ga_{0.74}In_{0.26}Sb$ superlattice on (111) GaSb substrate at a) 300 and b) 77 K.

3.3 Achieving VLWIR Superlattices

To extend the superlattice absorption edge to longer wavelengths we have investigated the $Ga_xIn_{1-x}Sb$/InAs superlattice growths on (111)A substrates by increasing the In composition in the alloy layer of the superlattice. As before, a GaSb buffer was first deposited. As the $Ga_xIn_{1-x}Sb$ alloy becomes more In-rich however, its lattice constant increases accordingly, and the overall balanced lattice constant of the superlattice no longer matches to the GaSb buffer underneath. We are concerned that additional defects resulting from the larger lattice mismatch would lead to inferior material quality. To circumvent this problem we experimented with an additional $Ga_yIn_{1-x}Sb$ alloy buffer on top of the GaSb. As demonstrated in Figures 10 and 11 the X-ray measurement verified that good $Ga_{0.85}In_{0.15}Sb$ ternary buffer can be deposited. The lattice constant of this buffer is chosen to be intermediate between those of the InAs and the alloy layers in the superlattice structure itself. This intermediate layer serves to shift the host lattice from GaSb to $Ga_yIn_{1-y}Sb$. Mismatch-related defects between the GaSb and the $Ga_xIn_{1-x}Sb$

$_x$Sb would be incorporated into this alloy buffer layer. It is anticipated that by growing this additional buffer to sufficient thickness, the superlattice will be smooth and uniform at the point of the superlattice deposition.

A superlattice sample of 80 pairs of $Ga_{0.52}In_{0.48}Sb$ (8 monolayers)/InAs (8 monolayers) was grown on this type of buffer structure. The superlattice maintained good quality throughout growth on this GaAs/buffers combination. The room temperature FTIR spectrum for this sample, displayed in Figure 17, indicates a cutoff wavelength of ~12 μm. This wavelength is longer than what has been observed in previous samples. It is therefore promising to build superlattice structures of progressively longer cutoff wavelengths on properly balanced buffer layers.

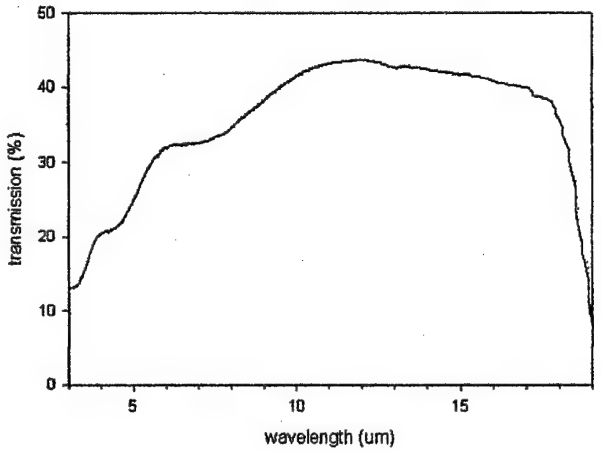

Figure 17. Transmission FTIR spectrum for an 80 pair superlattice consisting of $Ga_{0.52}In_{0.48}Sb$ (8 monolayers) / InAs (8 monolayers) using a $Ga_{0.85}In_{0.15}Sb$ buffer layer on (111A) GaAs substrate.

We attempted several variations on this theme. One example is a sample with as much as 70% In in the alloy layer of the superlattice, on top of a 36% InGaSb buffer. The total period is 90 and the thickness ratio if 5:7 ml of alloy to InAs. Transmission data were carried out at both the ambient and LN2 temperatures, as shown in Figure 18 (a) and (b),

respectively. Due to oscillation in the data it is inconclusive whether the bandedge transmission has extended further into the infrared.

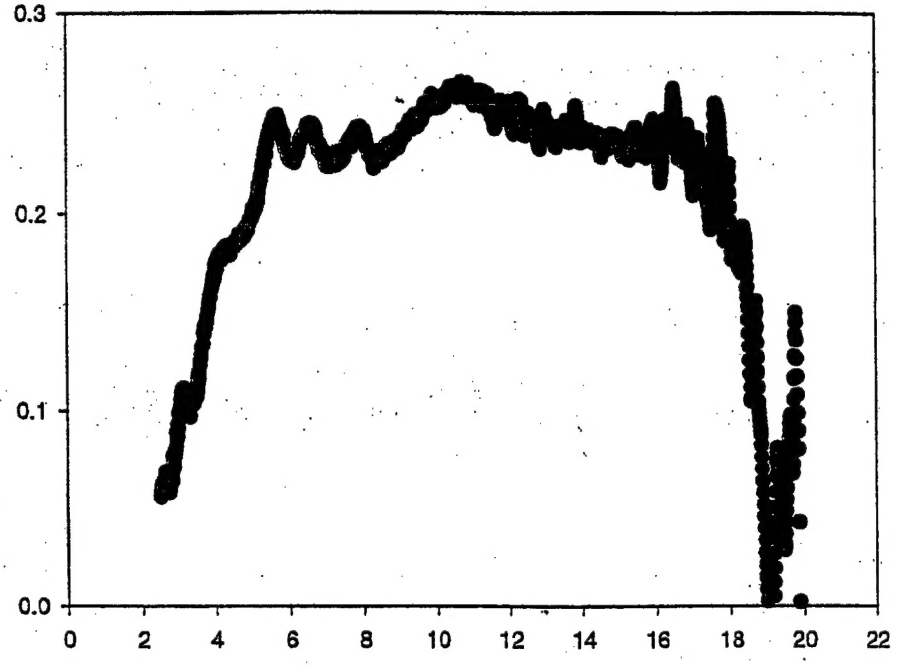

(a) Transmission vs wavelength measurement at ambient temperature.

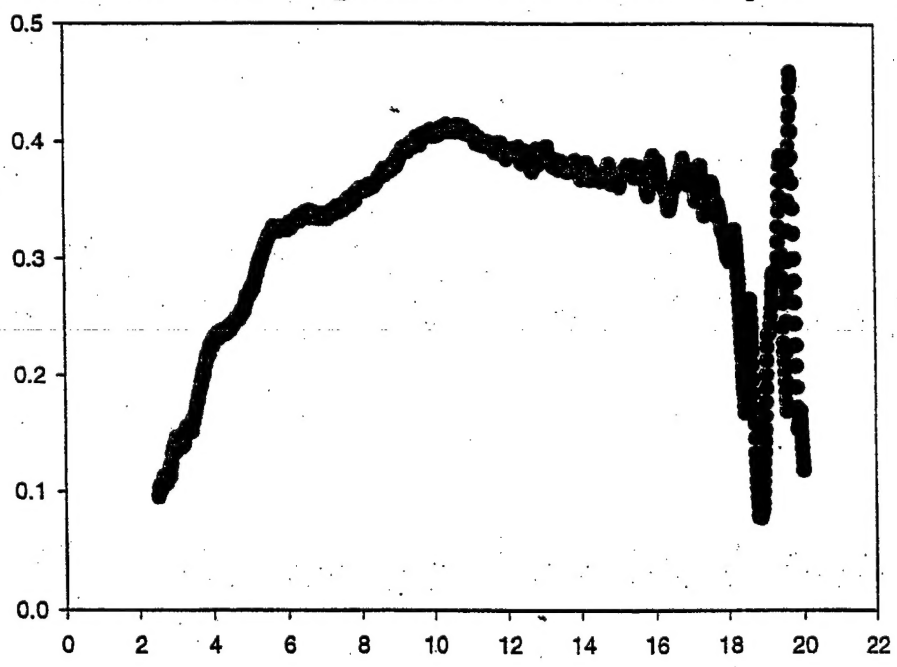

(b) Same measurement at 6°K.

Figure 18. Transmission measurement of 90x InAs/$In_{0.70}Ga_{0.30}Sb$ superlattice on $In_{0.36}Ga_{0.64}Sb$ and GaSb buffers on (111)A GaAs. The thickness ratio is 5:7 ml InGaSb to InAs. (a) ambient, and (b) 6°K.

A second approach to balance the strain is to vary the thickness ratio of the InAs and $Ga_xIn_{1-x}Sb$ in the superlattice. Many samples studied in this project were made to have equal thickness of the two layers while only the In-content was varied, such that the change in bandedge may be easier to discern. The disadvantage of equal layer thickness is that the overall strain is not balanced, resulting in higher defect in the structures. One example of thickness variation is shown in Figure 18 where the ratio of the two layers is 5:7. Extending the ratio of about 2:1 would in principle result in overall structural balance and only GaSb layer would suffice to provide a good buffer for superlattice growth. A series of this type of superlattice samples have been investigated. The results shown in the following two figures are on a sample of 50 periods 20:8 InAs/$In_{0.25}Ga_{0.75}Sb$ superlattice on a GaSb buffer layer. The RHEED pattern during growth remained streaky and the X-ray diffraction in Figure 19 exhibits reasonable quality.

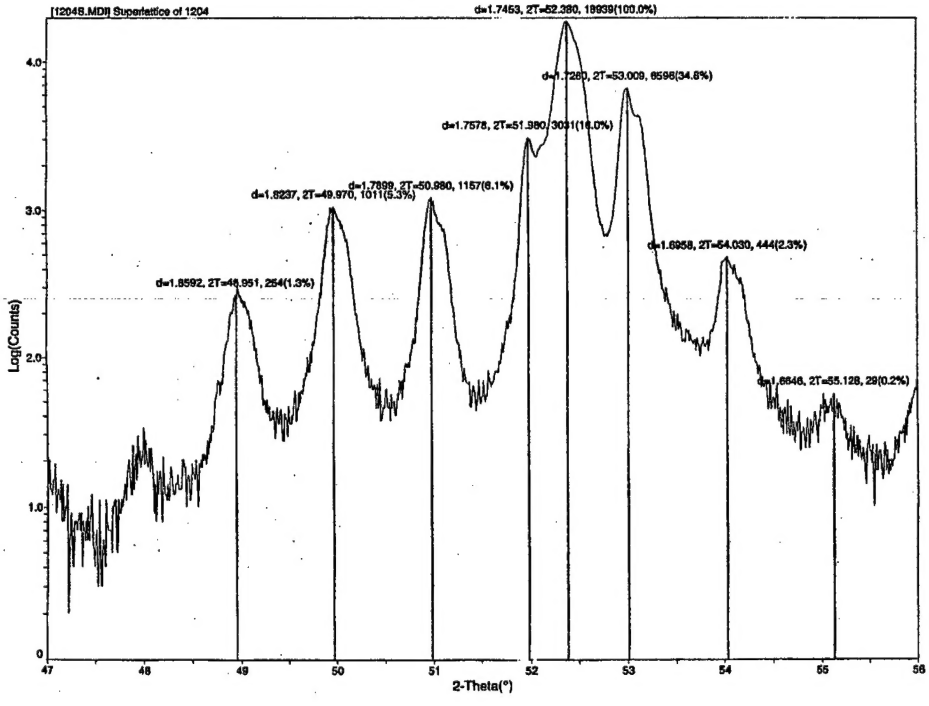

Figure 19. X-ray diffraction of a InAs/$In_{0.25}Ga_{0.75}Sb$ superlattice on (111) A GaAs through a GaSb buffer layer.

The FTIR measurement of the sample is displayed in Figure 20 showing a 15 μm bandedge transmission. This represents the smallest superlattice bandedge of all the samples investigated during this project. An alloy sample of similar composition is also shown for reference.

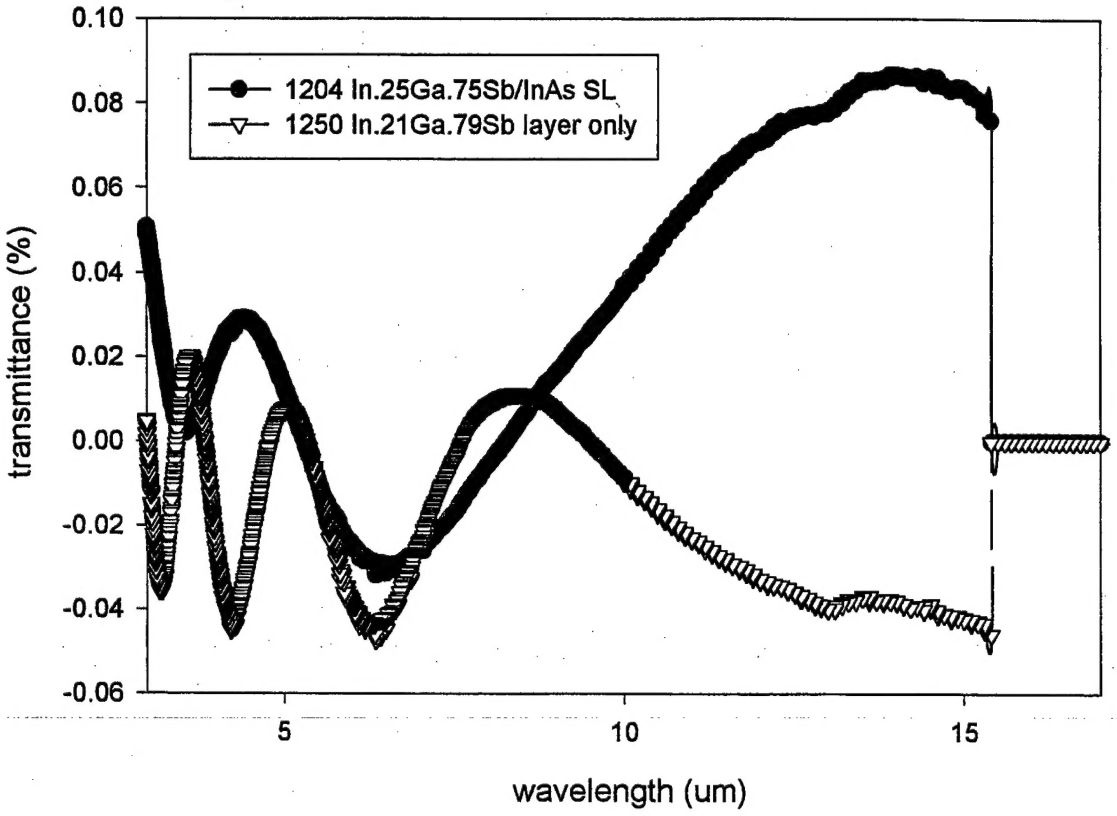

Figure 20. FTIR measurement of the same sample showing 15 μm bandedge transmission. That of an alloy sample of the same composition is also shown for comparison. The alloy composition $In_{0.25}AsSb$ grown on GaSb buffer.

4.0 Summary Conclusion

We have carried out a large number of growth runs in order to investigate the potential of (111) InAs/InGaSb superlattices for VLWIR applications. Due to lack of availability of suitable GaSb substrates our strategy has been to make suitable buffer layers on the semi-insulating GaAs substrates before the superlattices are grown. This strategy has made possible not only the fabrication of these superlattices but also their optical and electrical characterizations.

Although significant progress was made to produce reasonable quality (111) superlattice samples, further improvement is necessary to reach the level of the (100) superlattices. Interpretation of the measurement result is thus in part affected by the relatively high level of defects in these samples, and decisive comparison can not yet be made between the two crystalline orientations. Nonetheless a systematic study has been carried out which resulted in producing bandedge transmission as long as 15 μm. Many samples exhibiting 8-12 μm have been demonstrated. We are hopeful with improving growth techniques the theoretical prediction for these (111) superlattices may be realized.